Article ID: 1000-324X(2017)05-0555-06 **DOI:** 10.15541/jim20160464

Effects of La Doping on CaB_6 Thin Films Prepared by DC Magnetron Sputtering

ZHANG Lin, LIU Hui-Hui, LIU Lin-Jia, ZHAO Guo-Qing, WU Yan, MIN Guang-Hui

(Key Laboratory for Liquid-Solid Structural Evolution and Processing of Materials (Ministry of Education), Shandong University, Jinan 250061, China)

Abstract: Both La doped and undoped $Ca_{1-x}La_xB_6$ (x = 0, 0.01, 0.02, 0.03) thin films were prepared by direct current magnetron sputtering method. Morphology and thickness of these films were characterized by atomic force microscopy. Thicknesses of doped films were about twice that of the undoped films, while the grain growth of the film was much enhanced by La doping. X-ray photoelectron spectroscopy (XPS) was used for investigating the chemical composition of film surfaces. Calculated La/Ca atomic ratios were close to the theoretical values, and there were no other ferromagnetic impurities or elements especially iron existing in films. $Ca_{0.98}La_{0.02}B_6$ films exhibited the highest room temperature saturation magnetization 84.54 emu/cm^3. The saturation magnetization decreased with increasing film thickness. B_6 vacancies may be the main source of magnetism. Other defects such as grain boundaries also affected the magnitude of magnetism.

Key words: CaB_6; thin film; La doping concentration; magnetism

The divalent alkaline earth hexaboride CaB_6 has a simple CsCl type structure. It is a candidate semiconductor material[1-2] for spin electronics with a band gap of 0.8 eV approximately. Since high temperature weak ferromagnetism[3] has been reported, CaB_6 has aroused numerous attentions both in the experimental and calculation fields. It suggested that the weak ferromagnetism is originated from dilute electron gas[3-4], the result of exotic phase[5-6] or excitonic state[7-8]. Intrinsic defects[9-11] were also been considered to give rise to the special magnetic property. Lofland[11] reported that defects not only enhanced the magnetic moment but also increased the ordering temperature. In addition, Monnier[9] found that only B_6 vacancy carried the magnetic moment in all intrinsic point defects.

The magnitude of the magnetism immensely depends on films morphology, microstructure and chemical composition[12]. Changes of the concentration of La doping in a small scale can cause dramatic magnetic changes[3]. We have investigated the growth evolution of CaB_6 films[13], and found out the relationship between film structure and magnetism[14].

The aim of this work is to build correlations between the concentration of La doping, films morphology, phonon vibration and magnetism. Then the mechanism of the magnetism is investigated. Films were prepared by direct current (DC) magnetron sputtering method, which is a nonequilibrium growth process. Sputtered films are generally formed by nanometer sized crystallites which have a special disorder[12], many defects and grain boundaries. Therefore, this method is suitable for fabricating defective nanostructure materials.

1 Material and methods

$Ca_{1-x}La_xB_6$ films (x=0, 0.01, 0.02, 0.03) were fabricated by DC magnetron sputtering system (FJL560C3, Shenyang Scientific Instruments Research Institute, China). CaB_6 micron powders with particle size of about 5 μm) were synthesized in a vacuum resistance furnace, and the detailed information of experimental and morphology can be obtained from reference [15]. La powders (nominal purity 99.95%) and silicon were directly got purchased. Before being sintered into targets, the CaB_6 powders were washed by hydrochloric acid to remove potential iron contaminants. Targets were fabricated by vacuum hot pressure sintering furnace with a mixture of CaB_6 and La powders according to reference [16]. Substrates were 20 mm×20 mm×0.35 mm slices of single-crystal Si (100) which were cleaned by successive processes in ethanol, acetone and ethanol. The target-substrate distance was 55 mm. Deposition parameters were selected according to our previous work[14]. The background pressure was kept at 6×10^{-4} Pa. The flow rate of Ar was 25 sccm and the argon pressure was main-

Received date: 2016-08-10; **Modified date:** 2016-09-09
Foundation item: National Natural Science Foundation of China (51102154), Fundamental Research Funds of Shandong University (2015JC033)
Biography: ZHANG Lin(1980–), female, associate professor. E-mail: zhanglin2007@sdu.edu.cn

tained at 1.0 Pa. The deposition power was 90 W and a –100 V bias voltage was applied. Pre-sputtering of 15 min was needed to remove impurities.

Film surface morphology and thickness were measured by atomic force microscopy (Dimension Icon). Average values of the interface width (σ) and roughness were obtained by the nanoscope analysis. Surface chemical composition was examined by X-ray photoelectron spectroscopy (Escalab-250). Atomic ratios *Cx* were calculated from peak area sensitivity factors through

$$Cx = \frac{N_x}{\Sigma_i N_i} = \frac{I_x / S_x}{\Sigma_i I_i / S_i} \quad (1)$$

N stands for the number of atoms and *I* is the peak area. Values of *S* based on peak area measurements are provided by the instrument manufacturer[17]. Field-emission scanning microscopy (SU-70 Hitachi) equipped with energy dispersion spectroscopy was also used to characterize film morphology and chemical composition. To analyze the effect of La doping concentration on lattice vibration frequencies, Raman scattering spectra (JYLabramHR800) was detected. Magnetization parameters were collected by an alternating gradient magnetometer (MicroMag 2900/3900) at room temperature. Samples were cut into 4 mm× 2 mm square shape and films were perpendicular to the applied magnetic field.

2 Results and discussion

2.1 Chemical composition analysis

XPS was applied to characterize chemical composition in the surface of $Ca_{1-x}La_xB_6$ films (x=0, 0.01, 0.02, 0.03). The XPS results were presented in Table 1. It was obvious that the concentration of La doping was close to the stoichiometric values. This indicates that La atoms have been successfully incorporated into the film. The Table 1 also indicated that B atoms were insufficient in films. It might be caused by differences of vaporization activation energy[18] between B, Ca and La atoms. Both EDS and XPS studies detected no ferromagnetic impurities (*eg*. Fe) existed in films.

2.2 Raman spectra analysis

Figure 1 showed the Raman spectra of $Ca_{1-x}La_xB_6$ films (x=0, 0.01, 0.02, 0.03) measured at room temperature.

Table 1 Atomic ratio in $Ca_{1-x}La_xB_6$ films

La doping concentration, x	Theoretical			Experimental		
	B	Ca	La	B	Ca	La
0	6	1	0	5.11	1	0
0.01	6	0.99	0.01	5.43	0.99	0.0077
0.02	6	0.98	0.02	4.63	0.98	0.0160
0.03	6	0.97	0.03	5.07	0.97	0.0300

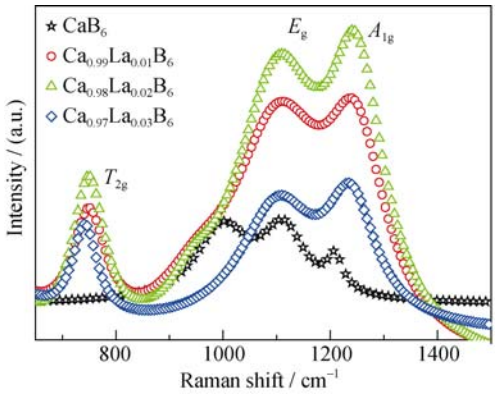

Fig. 1 Raman spectra of $Ca_{1-x}La_xB_6$ (x=0, 0.01, 0.02, 0.03) films

There were three single phonon peaks around 750 cm^{-1}(T_{2g}), 1100 cm^{-1}(E_g), 1220 cm^{-1}(A_{1g}), respectively. Peaks around 1000 cm^{-1} were identified as the silicon phonon vibration peaks[19]. Silicon peaks were so strong that the T_{2g} peaks could not be detected in CaB_6 films. In La doped films, E_g modes became broad and the frequency slightly decreased, and A_{1g} modes clearly turned into higher frequencies. A_{1g} peaks of $Eu_{1-x}La_xB_6$[20] showed an abrupt shift at low level of La doping as well. The change may be caused by the tilting or rotating of the B_6 in La doped films. Atomic radius differences between La and Ca could cause the tilting or rotating[20]. The slight decrease of E_g mode intensity was mainly attributed to the decreasing strength of inter-octahedral B–B bonds[21]. This may also be caused by a larger atomic radius of La. Raman intensity increased in the order x=0, 0.03, 0.01, 0.02. This indicated that the electronic polarizability increased in the same order, because the intensity of Raman scattering is directly proportional to the electronic polarizability[22].

2.3 Morphology and growth evolution

Figure 2(a) and 2(b) demonstrated the surface morphologies of $Ca_{1-x}La_xB_6$ (x=0, 0.01, 0.02, 0.03) films with the same deposition time (60 min). Compared with undoped films, particles in La doped films were very uniform. When the doping concentration x=0.03, particles were slightly smaller than x=0.02. In Fig. 2(c) and Fig. 3(a), it was clear that thickness of doped films was nearly two times as big as the undoped films. The approximate values of growth rate for $Ca_{1-x}La_xB_6$(x=0, 0.01, 0.02, 0.03) films were 11.05, 18.95, 18.78 and 18.17 nm/min, respectively. Therefore, grain growth was much enhanced by La doping. The values of film growth rate did not change significantly with La doping concentrations.

Bearing analysis indicated the percentage of the surface lies above or below the threshold value. It can reveal the height distribution over the surface[23]. In Fig. 3(b), the curve of La doped films moved to the right. With the concentration of La doping increasing, the average height of

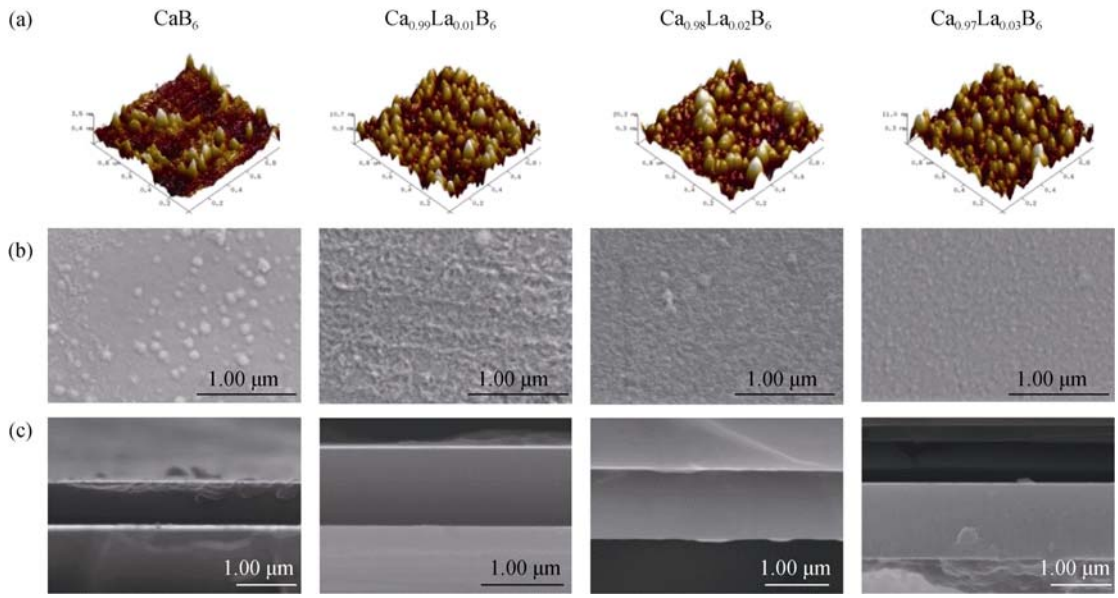

Fig. 2　(a) AFM surface morphologies, (b) FESEM images and (c) cross section morphologies of $Ca_{1-x}La_xB_6$ films deposited for 60 min

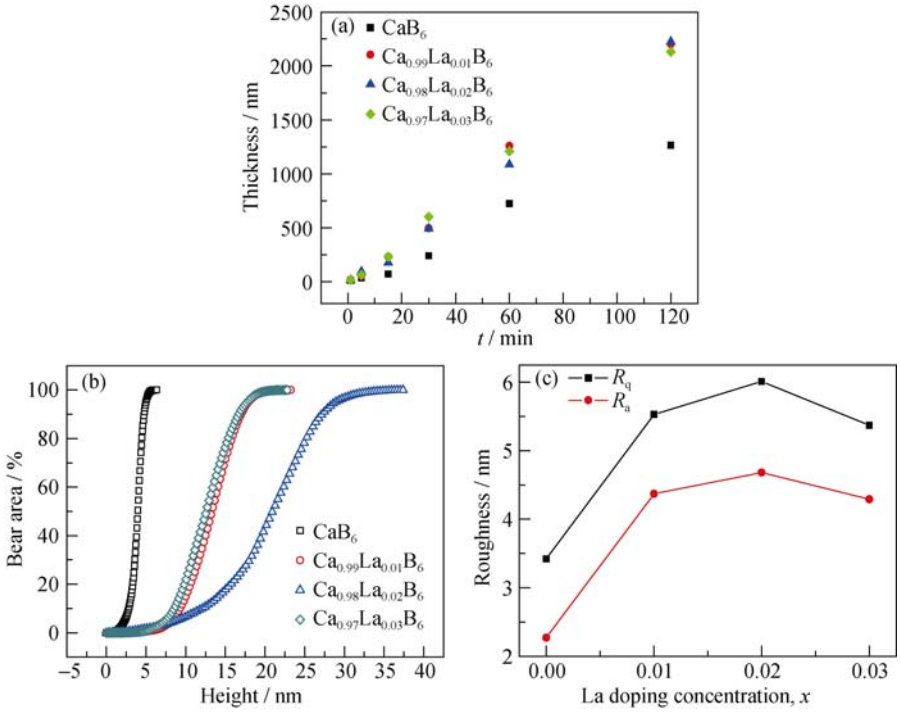

Fig. 3　(a) Film thickness, (b) bearing analysis and (c) R_q and R_a roughness of $Ca_{1-x}La_xB_6$ (x=0, 0.01, 0.02, 0.03) films
In (b) and (c) films were deposited for 60 min

particles in the film surface rose from ~5 nm to ~30 nm. However, height distributions in $Ca_{0.97}La_{0.03}B_6$ films became narrower and smaller than $Ca_{0.98}La_{0.02}B_6$ films, which was close to the $Ca_{0.99}La_{0.01}B_6$ films. It may attribute to the refinement effect on the growth of excessive La atoms. Root-mean-square roughness (R_q) and mean roughness (R_a) were calculated by AFM analysis. The dependence of roughness on the concentration of La doping was shown in Fig. 3(c). R_q and R_a value grew with the increase of La doping concentration. However, roughness value of $Ca_{0.97}La_{0.03}B_6$ film was smaller than that of $Ca_{0.98}La_{0.02}B_6$ film. R_q and R_a values followed a similar change tendency, and were in accordance with the microscopic observations as well as results displayed in Fig. 3(b).

In order to investigate the growth dynamics, the interface width σ and growth exponent β were calculated from section analysis by AFM software. Fig. 4 demonstrated the evolution of σ with the sputtering time and the calculated value of β. The evolution of interface width σ was roughly according to a power law based on time. $Ca_{1-x}La_xB_6$ (x=0, 0.01, 0.02, 0.03) films were characterized by the exponents β, which equal to 0.53±0.06, 0.53±0.08, 0.51±0.08

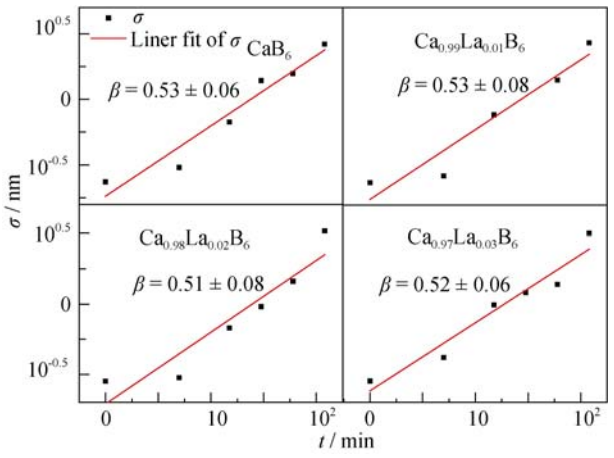

Fig. 4 The interface width σ of $Ca_{1-x}La_xB_6$films measured from AFM image *versus* deposition time and calculated values of the exponent β

and 0.52±0.06. The value was consistent with the result we reported earlier[13]. This illustrated that La doping didn't change the growth dynamic of $Ca_{1-x}La_xB_6$ films. Furthermore, the balance between shadowing effect and smoothing was not affected by the concentration of La doping.

2.4 Magnetic property

Figure 5 showed the room temperature magnetization curves for $Ca_{1-x}La_xB_6$ films with different thicknesses after the Si substrate signal was subtracted, and field was applied perpendicular to the films. All curves exhibited typical hysteresis loops for ferromagnetic materials with coercive field about 70 Oe. Variation of $Ca_{0.98}La_{0.02}B_6$ films magnetization with film thickness is shown in Fig. 6. As the result showed in our previous work[14], there was a clear drop of the saturation magnetization (M_s) with the rise of sputtering time. Similar phenomenon was observed in the other $Ca_{1-x}La_xB_6$ (x=0, 0.01 and 0.03) films. The saturation magnetization for x=0, 0.01, 0.02 and 0.03 films (t~20 nm) were 6.43, 17.17, 84.54 and 15.26 emu/cm^3, respectively. Elsewhere it was reported[3] that $Ca_{0.995}La_{0.005}B_6$ had the largest magnetic moment. The value of M_s was much higher than that in Ref [3]. The variation of M_s with La doping concentration follows a similar trend. Sputtered films can possess many grain boundaries and defects. Lofland[11] has proposed that defects could enhance the magnetic moment.

There was a clear relationship between structure and magnetic property. The saturation magnetization Ms increased in the order x=0, 0.03, 0.01, 0.02, as well as roughness, average height and electronic polarizability. In the calculations of Monnier[9], only B_6 vacancy carried a large magnetic moment. Maiti[24] suggested that the B_6 vacancy give rise to the formation of an impurity band nearly on the Fermi level, and the exchange splitting of impurity states will result in a magnetic moment. B vacancy was very likely to exist in our $Ca_{1-x}La_xB_6$ films, due to the insufficiency B atoms. The Raman shift indicated that there was a tilting or rotating of the B_6 and a change between the bond energy of B–B. It may hence be tentatively suggested that B_6 vacancy or other B vacancy play an important role in the unexpected ferromagnetism of $Ca_{1-x}La_xB_6$ films. As reported by Monnier[9], when the La concentration was low (x=0.01), the incorporation of La would increase the possibility of the formation of B_6 vacancies. With increased La doping concentration (x=0.02), some Ca atoms would be replaced by La atoms and the magnetic moment would still grow. If the concentration was too high (x=0.03), La atoms would start to occupy B_6 vacancies and then the magnetic moment would decline.

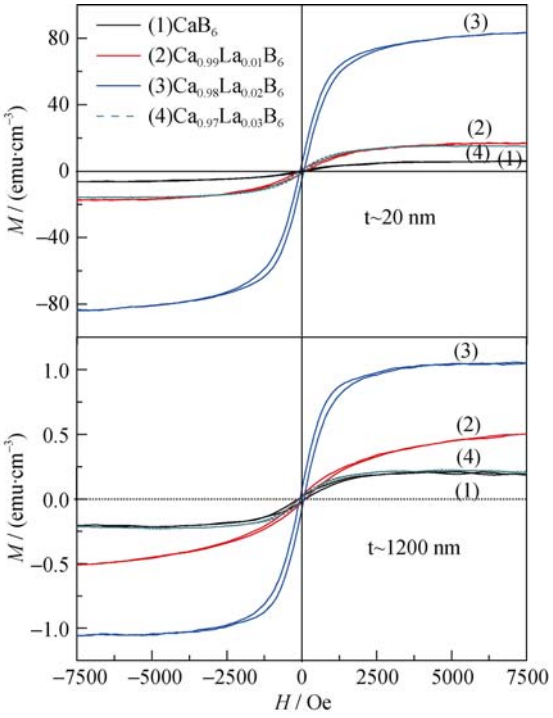

Fig. 5 Room temperature magnetization curves for thick (t~1200 nm) and thin (t~20 nm) La doped CaB_6 films
[Oe=(1000/4π)A·m^{-1}; emu·cm^{-3}=4π×10^{-4} Wb·cm^{-3}]

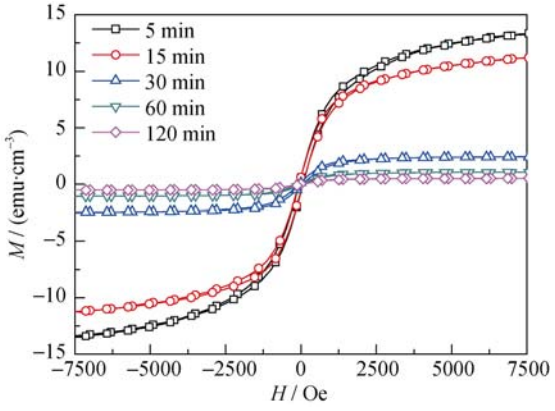

Fig. 6 Room temperature magnetization curves for $Ca_{0.98}La_{0.02}B_6$ films with different sputtering times
[Oe=(1000/4π)A·m^{-1}; emu·cm^{-3}=4π×10^{-4} Wb·cm^{-3}]

While other ferromagnetic materials especially Fe[5], which may be merged into the film during the sputtering process or other procedures in the experiments[5], has been considered as the origin of the magnetism. However, our results indicated that the magnetism was not caused by iron. Assuming that the iron was incorporated during the sputtering process, the saturation magnetization would be expected to increase with the increase of film thickness or deposition time. While both La doped and undoped films exhibited the same law (a sample displayed in Fig. 6), the thinnest film had the greatest saturation magnetization. EDS and XPS analysis of $Ca_{1-x}La_xB_6$ films did not detect any iron impurities with the detection sensitivity at about 0.1at%. In our previous work[14], there was no obvious change of the Ms value before and after the acid treatment. Therefore, the magnetism was an intrinsic feature of the $Ca_{1-x}La_xB_6$ films, not originated from other elements.

3 Conclusions

The effects of La doping concentration on morphology, Raman spectra and magnetic properties of $Ca_{1-x}La_xB_6$ films deposited by DC magnetron sputtering method were analyzed in this paper. Thickness of doped films was nearly as two fold as that of the undoped films with the same deposition time, and the grain growth of the film was much enhanced by La doping. But La doping has not changed the growth dynamic of $Ca_{1-x}La_xB_6$ films. The value of roughness, average height and electronic polarizability increased in the same order x=0, 0.03, 0.01, 0.02, as well as the saturation magnetization M_s. The largest value of M_s 84.54 emu/cm^3 appeared in $Ca_{0.98}La_{0.02}B_6$ films. B_6 vacancy or other B vacancy played an important role in the unexpected ferromagnetism of $Ca_{1-x}La_xB_6$ films. Other types of defects also affected the magnetic property. The relationship between the number and type of defect and magnetic moment is still undefined. It is necessary to find a controllable method to study the special magnetism.

References:

[1] LEE BYOUNGHAK, WANG LIN-WANG. Electronic structure of calcium hexaborides. *Appl. Phys. Lett.*, 2005, **87(26):** 262509.

[2] SOUMA S, TAKAHASHI T. Fermi surface of novel borides: MgB_2 and CaB_6. *J. Phys. Condens.*, 2007, **19(35):** 355003.

[3] YOUNG D P, HALL D, TORELLI M E, *et al*. High-temperature weak ferromagnetism in a low-density free-electron gas. *Nature*, 1999, **397:** 412–414.

[4] CEPERLEY DAVID. Condensed-matter physics: return of the itinerant electron. *Nature*, 1999, **397:** 386–387.

[5] MATSUBAYASHI K, MAKI M, TSUZUKI T, *et al*. Magnetic properties (communication arising): parasitic ferromagnetism in a hexaboride? *Nature*, 2002, **420:** 143–144.

[6] MORI TAKAO, SHIGEKI OTANI. Ferromagnetism in lanthanum doped CaB_6: is it intrinsic? *Solid State Commun.*, 2002, **123(6/7):** 287–290.

[7] ZHITOMIRSKY M E, RICE T M, ANISIMOV V I. Magnetic properties: ferromagnetism in the hexaborides. *Nature*, 1999, **402:** 251–253.

[8] MURAKAMI SHUICHI, SHINDOU RYUICHI, NAGAOSA NAOTO, *et al*. Theory of excitonic states in CaB_6. *Phys. Rev. B*, 2002, **66(18):** 184405.

[9] MONNIER R, DELLEY B. Point defects, ferromagnetism, and transport in calcium hexaboride. *Phys. Rev. Lett.*, 2001, **87(15):** 157204.

[10] SAKURABA Y, KATO H, SATO F, *et al*. Anisotropic lattice expansion and magnetism in sputter-deposited Ca(La)B_6 films. *Phys. Rev. B*, 2004, **69(14):** 140406.

[11] LOFLAND S E, SEAMAN B, RAMANUJACHARY K V, *et al*. Defect driven magnetism in calcium hexaboride. *Phys. Rev. B*, 2003, **67(2):** 020410.

[12] LESLIE-PELECKYD DIANDRA L, RIEKE REUBEN D. Magnetic properties of nanostructured materials. *Chem. Mater.*, 1996, **8(8):** 1770–1783.

[13] LIU HUI-HUI, ZHANG LIN, ZHAO GUO-QING, *et al*. Growth evolution of CaB_6 thin films deposited by DC magnetron sputtering. *Ceram. Int.*, 2015, **41(6):** 7745–7750.

[14] ZHAO GUO-QING, ZHANG LIN, HU LI-JIE, *et al*. Structure and magnetic properties of nanocrystalline CaB_6 films deposited by magnetron sputtering. *J. Alloys Compd.*, 2014, **599:** 175–178.

[15] ZHANG LIN, MIN GUANG-HUI, YU HUA-SHUN. Reaction mechanism and size control of CaB_6 micron powder synthesized by the boroncarbide method. *Ceram. Int.*, 2009, **35(8):** 3533–3536.

[16] ZHANG LIN, MIN GUANG-HUI, YU HUA-SHUN. Morphology characteristics and mechanical properties of nano/micron calcium hexaboride sintered body. *J. Inorg. Mater.*, 2010, **25(1):** 87–90.

[17] ZUYDERHOFF EMILIENNE M, DEKEYSER CAROLINE M, ROUXHET PAUL G, *et al*. An AFM, XPS and wettability study of the surface heterogeneity of PS/PMMA-r-PMAA demixed thin films. *J. Colloid Interface Sci.*, 2008, **319(1):** 63–71.

[18] CRACIUN V, CRACIUN D. Pulsed laser deposition of crystalline LaB_6 thin films. *Appl. Surf. Sci.*, 2005, **247(1):** 384–389.

[19] SCHMIDT MICHAEL STENBŒK, HÜBNER JÖRG, BOSIEN ANJA. Large area fabrication of leaning silicon nanopillars for

surface enhanced ramanspectroscopy. *Commun.: Adv. Opt. Mater.*, 2012, **24(10):** OP11–OP18.

[20] SONG M, YANG IN-SANG, SEO C W, *et al*. Local symmetry breaking in $Eu_{1-x}La_xB_6$. *J. Magn. Magn. Mater.*, 2007, **310(2):** 1019–1020.

[21] WERHEIT H, VOLODIMIR FILIPOV. Raman effect in boron and boron-rich compounds. *Boron Rich Solids*, 2010, 29–43.

[22] PERSSON B N J, ZHAO KE, AND ZHANG ZHEN-YU. Chemical contribution to surface-enhanced Raman scattering. *Phys. Rev. Lett.*, 2006, **96(20):** 207401.

[23] WU YAN, MIN GUANG-HUI, CHEN DE-FANG, *et al*. The correlation of stoichiometry between boron-rich LaB_6 targets and LaB_6 films. *Ceram. Int.*, 2015, **41(1):** 1005–1013.

[24] MAITI KALOBARAN. Role of vacancies and impurities in the ferromagnetism of semiconducting CaB_6. *EPL-Europhys. Lett.*, 2008, **82(6):** 67006.

La 掺杂对磁控溅射 CaB_6 薄膜的影响

张 琳, 刘慧慧, 刘林佳, 赵国庆, 吴 艳, 闵光辉

(山东大学 材料液固结构演变与加工教育部重点实验室, 济南 250061)

摘 要: 利用直流磁控溅射的方法制备掺 La 和未掺 La 的 $Ca_{1-x}La_xB_6$ (x = 0, 0.01, 0.02, 0.03)薄膜。利用原子力显微镜对薄膜的表面形貌及厚度进行表征。掺 La 的薄膜的厚度约为未掺杂的两倍; La 的掺杂会使薄膜的晶粒尺寸变大。利用 X 射线光电子能谱对薄膜表面的化学组成进行检测。薄膜中 Ca/La 比接近理论值, 没有检测到其它的铁磁性杂质及元素, 尤其是 Fe。$Ca_{0.98}La_{0.02}B_6$ 薄膜具有最大的室温饱和磁化强度, 强度值为 84.54 emu/cm^3。同时薄膜的饱和磁化强度值随薄膜厚度的增加而降低。在 $Ca_{1-x}La_xB_6$ 薄膜中, B_6 空位是薄膜磁性的主要来源, 其它类型的缺陷例如晶界等, 同样影响着薄膜磁性的大小。

关 键 词: CaB_6; 薄膜; La 掺杂量; 磁性

中图分类号: TB321 **文献标识码:** A